# A Rendez-vous in Time: Frequency-Domain Precoding for LoS Alignment in Distributed MISO

Thibaut Rolland*†, Matthieu Crussière†, Marie Le Bot*,
*Orange Innovation, 4 Rue du Clos Courtel, 35510 Cesson-Sévigné, France
{thibaut.rolland, marie.lebot}@orange.com
†IETR/INSA Rennes, 20 Avenue des Buttes de Coësmes, 35708 Rennes Cedex 7, France
{thibaut.rolland, matthieu.crussiere}@insa-rennes.fr

***Abstract*—This paper investigates the impact of Line-of-Sight (LoS) path misalignment in distributed Multiple-Input Single-Output (MISO) systems, particularly in millimeter-wave (mmWave) bands where phase synchronization and timing precision are critical. The goal is to validate a bit error rate model under practical OFDM transmission scenarios involving multiple access points communicating with user equipment. We highlight how time misalignment between LoS paths can degrade system performance and evaluate the effectiveness of various compensation strategies under such conditions. A key contribution of this work is the proposed compensation technique for LoS path misalignment. By applying a frequency-dependent linear phase shift to each subcarrier—an operation that is both low in complexity and easy to implement—we induce a circular rotation of the OFDM time-domain symbol. This rotation effectively aligns the various LoS contributions in time, as long as the path delays remain within the cyclic prefix duration. Notably, the method is fully compatible with analog beamforming architectures, which are essential in mmWave systems to reduce the number of costly RF chains. As a result, the proposed strategy enables efficient time compensation with minimal computational and hardware overhead, making it particularly attractive for distributed Multiple-Input Multiple-Output (MIMO) deployments at mmWave frequencies.**

## I. Introduction

Aligning line-of-sight (LoS) paths in a distributed MIMO network is a crucial challenge for enhancing system capacity and robustness. Several studies have investigated the impact of LoS links in centralized and distributed MIMO architectures, yet few have specifically explored strategies for aligning these paths across multiple access points (APs). Research on distributed MIMO, such as [1], [2], highlighted the potential of spatial multiplexing in networks where multiple antennas cooperate to improve coverage and signal diversity. Other studies, such as [3], [4], introduced precoding schemes tailored for LoS environments, leveraging channel correlation to maximize spatial gain. However, most existing approaches focus on scenarios where LoS links are either not actively exploited or treated as a limitation rather than a potential advantage.

In the domain of mmWave and sub-THz communications, some authors [5], [6] have proposed beamforming strategies tailored for highly directive environments, enabling better exploitation of dominant LoS links. However, these techniques are often limited to scenarios involving a single AP, lacking coordination across multiple distributed nodes. Other contributions [7], [8] have explored AP selection optimization in distributed MIMO systems, but without explicitly addressing the LoS alignment across APs. Yet, such alignment is a key challenge in distributed MIMO architectures, especially at high frequencies where LoS paths dominate due to severe path loss and limited diffraction. Coherently combining LoS components from multiple APs offers significant benefits, including increased spectral efficiency through enhanced received power, improved coverage via spatial diversity, and greater reliability by mitigating the effects of fading and blockage through constructive signal alignment.

Our work distinguishes itself by proposing an optimized LoS path alignment methodology in a distributed MIMO configuration, significantly enhancing spatial gain and transmission robustness. This technique is made feasible by the cyclic prefix (CP) in the OFDM waveform, which effectively mitigates inter-symbol interference (ISI) and preserves orthogonality across subcarriers. As a result, the channel frequency response remains flat, ensuring consistent performance across the transmission bandwidth. Importantly, the proposed strategy operates without the need for a central processing unit to perform precoding, as each AP independently applies its own precoding based on its knowledge of the channel and where its LoS path must temporally align with the others at the receiver. Moreover, the system is resilient to blockage: if one or more APs become obstructed, the remaining ones can continue to align their paths and contribute to the received signal coherently. However, the equalizer at the receiver must be adapted accordingly to adjust the combining threshold and avoid relying on the contribution of the blocked paths.

Thus, our approach fills a gap in the state of the art by introducing a novel way to exploit LoS paths in distributed MIMO networks. It paves the way for various applications, particularly in future 6G networks and high-density communication environments.

## II. Distributed MISO System and Channel Model

The considered distributed network is a multipoint-to-point system comprising a set $\mathcal{S}$ of $K_{\mathcal{AP}}$ APs, synchronously transmitting a common signal to a UE. This setup allows the UE to receive a superposition of signals from different channels. Each AP is equipped with $N_{Tx}$ antenna elements (AEs) arranged in the YZ-plane of the local coordinate system (LCS), forming a uniform rectangular array (URA) with AE

979-8-3503-9281-4/25/$31.00 ©2025 IEEE

spacing of $\lambda_0/2$, where $\lambda_0$ is the wavelength of the transmitted signal. These AEs have either omnidirectional or specific radiation patterns.

### A. Multipoint-to-Point Channel Model

The downlink channel impulse response for each AP $k$ follows a tapped delay line model [9], with $N_r$ rays $m$ grouped into clusters $c$ based on similar arrival delays. Each ray is defined by departure angles $(\theta^{\text{ZoD}}_{k,c,m}, \phi^{\text{AoD}}_{k,c,m})$ and arrival angles $(\theta^{\text{ZoA}}_{k,c,m}, \phi^{\text{AoA}}_{k,c,m})$ in the global coordinate system (GCS). The orientation of the $k$th panel array relative to the GCS is defined by the angles $\alpha_k$, $\beta_k$, and $\gamma_k$, corresponding to successive rotations around the $Z$, $Y$, and $X$ axes. This coordinate system transformation is crucial for determining the AEs' positions and field expressions in the GCS (see [9] for details).

The position of the $i$th AE of the $k$th link in the GCS is denoted as $\mathbf{P}^{\text{Tx,k}}_i = \left(P^{\text{Tx,k}}_{i,x}, P^{\text{Tx,k}}_{i,y}, P^{\text{Tx,k}}_{i,z}\right)$. The path difference from the $i$th AE to the wave is computed as the scalar product between the position vector $\mathbf{P}^{\text{Tx}}_i$ and the ray direction vector $\mathbf{R}^{\text{Tx,k}}_{c,m}$, defined as: $\left(\sin\left(\theta^{\text{ZoD}}_{k,c,m}\right)\cos\left(\phi^{\text{AoD}}_{k,c,m}\right), \sin\left(\theta^{\text{ZoD}}_{k,c,m}\right)\sin\left(\phi^{\text{AoD}}_{k,c,m}\right), \cos\left(\theta^{\text{ZoD}}_{k,c,m}\right)\right)$. Thus, assuming a normalized cluster power $P^k_c$ equally spread across rays, the narrowband channel gain between the UE and the $i$th AE of AP $k$ at frequency $f$ relative to center frequency $f_0$ is $H^k_i(f)$:

$$\sqrt{\frac{K^k_r}{K^k_r+1}} g^{\text{Tx,k}}_{\text{LoS}} e^{j\frac{2\pi}{\lambda_0}\left(\mathbf{P}^{\text{Tx},k}_i \cdot \mathbf{R}^{\text{Tx},k}_{\text{LoS}}\right)} e^{-j2\pi(f_0+f)\tau^{k,i}_{\text{LoS}}} + \sqrt{\frac{1}{K^k_r+1}} \times \sum_{c\in\mathcal{C}^*_k}\sum_{m=1}^{N_r} \sqrt{\frac{P^k_c}{N_r}} g^{\text{Tx,k}}_{c,m} e^{j\frac{2\pi}{\lambda_0}\left(\mathbf{P}^{\text{Tx},k}_i \cdot \mathbf{R}^{\text{Tx},k}_{c,m}\right)} e^{-j2\pi(f_0+f)\tau^{k,i}_c} \quad (1)$$

where $\tau^{k,i}_{\text{LoS}}$ denotes the delay of the LoS path between the $i$th antenna element of AP $k$ and the UE, while $\tau^{k,i}_c$ represents the common delay associated with all rays in cluster $c$, relative to the $i$th antenna element. These delays account for both the 3D propagation distance and the spatial position of the antenna within the array. $g^{\text{Tx,k}}_{c,m}$ and $g^{\text{Tx,k}}_{\text{LoS}}$ are the complex gains depending on the polarized field components and initial phases of each ray. $\mathcal{C}_k$ is the set of the clusters of the $k$th AP's channel, with $\mathcal{C}^*_k = \mathcal{C}_k - \{0\}$ excluding the LoS component which comes as the first term in (1). Finally, the Ricean $K$-factor is defined as $K^k_r = P^k_{\text{LoS}} / \sum_{c\in\mathcal{C}_k} P^k_c$, set to zero in NLoS scenarios.

### B. Phase Term Decomposition in the LoS Channel

This subsection details the decomposition of the LoS component of the frequency-domain channel gain. Under the far-field approximation, the delay from the $i$th antenna element of AP $k$ to the receiver consists of a common distance term and a correction based on the projection of the antenna's position onto the propagation direction:

$$\tau^{k,i}_{\text{LoS}} = \frac{d_k - \mathbf{R}^{\text{Tx},k}_{\text{LoS}} \cdot \mathbf{P}^{\text{Tx},k}_i}{c} \quad (2)$$

where $d_k$ is the 3D distance between the center of the panel array of AP $k$ and the UE, and $c$ is the speed of light in free space. Inserting this expression into the LoS path contribution leads to the following decomposition, which highlights the distinct phase terms involved:

$$H^{k,i}_{\text{LoS}}(f) = \sqrt{\frac{K^k_r}{K^k_r+1}} |g^{\text{Tx,k}}_{\text{LoS}}| \underbrace{e^{j\angle g^{\text{Tx,k}}_{\text{LoS}}}}_{\text{[1] Initial phase}} \cdot \underbrace{e^{-j\frac{2\pi}{\lambda_0}d_k}}_{\text{[2] Static distance phase}} \cdot \underbrace{e^{-j2\pi f\frac{d_k}{c}}}_{\text{[3] Frequency delay phase}} \cdot \underbrace{e^{j\frac{2\pi}{\lambda_0}\mathbf{P}^{\text{Tx},k}_i \cdot \mathbf{R}^{\text{Tx},k}_{\text{LoS}}}}_{\text{[4] Spatial phase}} \cdot \underbrace{e^{j2\pi f\frac{\mathbf{P}^{\text{Tx},k}_i \cdot \mathbf{R}^{\text{Tx},k}_{\text{LoS}}}{c}}}_{\text{[5] Frequency spatial phase}} \quad (3)$$

The expression in (3) reveals five distinct phase terms. The static distance and frequency delay phases are linked to the propagation distance between the AP and the UE and vary across APs; their compensation is essential for coherent combining of LoS signals. The spatial and frequency spatial phases arise from the antenna's position within the array and are typically addressed through analog or hybrid beamforming. The initial phase term, related to the field orientation and initial offset, is generally constant. Among these components, two phase terms vary with frequency. While the frequency delay phase is critical and must be compensated to prevent misalignment between LoS paths, the frequency-dependent spatial term is often negligible in narrowband systems, but may become significant in wideband or large-array configurations. This structured decomposition enables a precise understanding of which phase components require compensation depending on the system architecture and serves as the basis for the subsequent analysis of compensation strategies.

## III. LoS Delay Misalignment: A Challenge in Distributed OFDM

In distributed multi-AP systems, LoS paths typically reach the UE at different times due to unequal propagation distances. As a result, it is uncommon for these paths to arrive simultaneously at the receiver. Whether this temporal misalignment affects performance depends on the time resolution at the UE, which is determined by the OFDM sampling frequency:

$$T_s = \frac{1}{\Delta f \cdot N_{\text{FFT}}} \quad (4)$$

where $\Delta f$ is the subcarrier spacing and $N_{\text{FFT}}$ is the FFT size. In a distributed deployment, the LoS propagation delay from AP $k$ to the UE is $\tau^k_{\text{LoS}} = \frac{d_k}{c}$, where $d_k$ is the 3D propagation distance. The maximum interarrival delay is:

$$\Delta t = \max_k\left(\tau^k_{\text{LoS}}\right) - \min_k\left(\tau^k_{\text{LoS}}\right) \quad (5)$$

To evaluate if the LoS paths from different APs are perceived as arriving simultaneously at the UE, the maximum interarrival delay $\Delta t$ is compared to the sampling interval $T_{\text{s}}$. If $\Delta t < T_{\text{s}}$, all LoS components fall within the same sampling bin and can be coherently combined. Otherwise, when $\Delta t \geq T_{\text{s}}$, the signals are sampled at different time instants, which may introduce temporal dispersion, frequency selectivity in the channel, and ultimately ISI across OFDM symbols if $\Delta t$ is greater than the CP duration ($T_{\text{CP}}$). Even though each AP contributes a dominant single LoS path, differences in arrival time translate into frequency-domain distortions across the

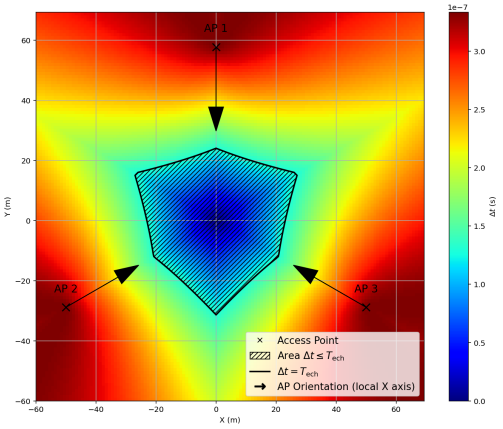


Figure 1: 2D map inter-arrival time $\Delta t$ with parameters $\Delta f = 15kHz$, $N_{\text{FFT}} = 512$, $T_s = 130ns$

OFDM subcarriers. Depending on the receiver design, a more conservative threshold such as $T_{\text{s}}/2$ may also be adopted.

This behavior is intrinsically linked to the coherence bandwidth of the resulting channel, which depends on the delay spread induced by the geometric distribution of the APs. In particular, the larger the differences in propagation delays between APs, the narrower the coherence bandwidth. While multipath effects within each link (e.g., reflections or local scattering) contribute modestly to the total delay spread, the dominant factor in LoS-dominated distributed systems remains the difference in LoS path lengths.

Thus, the composite channel in distributed MISO-OFDM systems exhibits frequency selectivity even under pure LoS conditions, solely due to geometric delay misalignment.

This behavior is visualized in Fig. 1, which displays a two-dimensional map of the deployment area. For each UE location, the maximum delay spread $\Delta t$ among LoS paths is evaluated and compared to the OFDM sampling interval $T_{\text{s}}$. The figure highlights regions where this condition is satisfied, using $N_{\text{FFT}} = 512$ and $\Delta f = 15$ kHz, yielding $T_{\text{s}} \approx 130$ ns. These parameters are chosen to illustrate a central region where LoS paths align temporally. However, in mmWave scenarios with 5G or 6G parameters—typically involving larger subcarrier spacing and FFT sizes—$T_{\text{s}}$ becomes significantly shorter, making such alignment regions more difficult to achieve. The APs are positioned at the vertices of an equilateral triangle with a side length of 100 meters.

## IV. Phase-Based Delay Compensation of LoS Paths

This section introduces a low-complexity frequency-domain technique designed to compensate for delay misalignment between LoS paths in distributed MISO-OFDM systems. Building upon the channel model and phase decomposition presented in Section II, the approach aims to restore coherent combining of LoS components by applying phase corrections that effectively realign their arrival times.

### A. Linear Phase Slope Correction: Motivation and Principle

In OFDM systems, a propagation delay $\tau$ introduces a frequency-dependent phase shift of $-2\pi f\tau$. In the distributed setup, each AP experiences a distinct LoS delay $\tau_{\text{LoS}}^k$ due to unequal distances to the UE. As shown in Section II, this results in a frequency-delay phase term $e^{-j2\pi f\tau_{\text{LoS}}^k}$ in the LoS component of the per-AP channel. To compensate for these delay differences, each AP applies a phase rotation before transmission to ensure that all LoS components arrive at the UE with the same effective delay. Let $\tau_{\text{ref}}$ denote the common reference delay targeted by all APs. The signal transmitted by AP $k$ after frequency-delay phase compensation is:

$$X_k^{[-3]}(f) = X(f) \cdot e^{j2\pi f(\tau_{\text{ref}} - \tau_{\text{LoS}}^k)} \tag{6}$$

where the superscript $^{[-3]}$ indicates that the phase component [3], corresponding to the frequency-dependent delay, has been neutralized. This operation aligns the LoS paths from all APs in time at the receiver, provided that the relative delays remain within the CP duration. It induces a circular rotation of the time-domain OFDM symbol, effectively applying a time advance of $\tau_{\text{LoS}}^k - \tau_{\text{ref}}$ seconds at AP $k$. Note that $\tau_{\text{ref}}$ does not need to match any specific $\tau_{\text{LoS}}^k$; it can be chosen arbitrarily as long as all APs compensate accordingly to ensure synchronous arrival. After this correction, the composite LoS channel exhibits flat phase evolution across subcarriers. However, for the LoS signals from different APs to add constructively, the static distance-dependent phase term [1], $e^{-j\frac{2\pi}{\lambda_0}d_k}$, must also be compensated. Once both the delay-dependent phase [2] and the static phase [1] are corrected, the LoS components become phase-aligned at the receiver. Ultimately, the overall received power can be maximized by additionally correcting the spatial phase [4], which corresponds to conventional beamforming.

### B. Practical Implementation in Distributed Architectures

Implementing the proposed delay compensation technique in practical distributed systems requires minimal coordination and is particularly well-suited to architectures without centralized processing. Each AP needs only to estimate its own LoS delay $\tau_{\text{LoS}}^k$ to the UE, which can be obtained through standard channel estimation procedures or inferred from location and geometry. Crucially, no AP needs knowledge of the channels or delay values of the other APs, nor does the system require a central unit to coordinate the corrections. This decentralized nature is a key advantage of the approach.

The correction is applied locally by each AP, which adjusts its transmission in the frequency domain by applying a phase rotation of $e^{j2\pi f(\tau_{\text{ref}} - \tau_{\text{LoS}}^k)}$, so that its LoS component arrives at the UE with an effective delay equal to the common reference $\tau_{\text{ref}}$. From the UE's perspective, the different LoS signals then "rendez-vous" in time, arriving aligned at the same sampling instant. This gives the method its name: the *rendez-vous algorithm*. Each AP targets the same temporal reference, aligns accordingly, and waits for the others to do the same—no signaling is needed between APs beyond time-frequency synchronization.

For analog beamforming, beam selection can be handled via beam sweeping procedures such as those based on synchronization signal blocks (SSBs), as specified in 5G NR. These blocks allow each AP to determine the best direction without

requiring global channel knowledge. Since each AP estimates only its own link and applies both delay compensation and beamforming weights locally, the overall system remains fully decentralized. This distributed execution, where each AP independently targets the same arrival time $\tau_{\text{ref}}$, encapsulates the "rendez-vous" principle underpinning the proposed approach.

### C. Impact and Advantages

The proposed delay compensation method offers several advantages in distributed OFDM systems. First, it is of low complexity, requiring only a per-subcarrier complex multiplication, making it computationally efficient. Since the phase rotation is deterministic and known, it preserves the amplitude of constellation symbols, ensuring their integrity. The technique is also fully transparent to the receiver, as all operations are performed at the transmitter side without requiring changes at the UE. Moreover, the correction is compatible with analog beamforming architectures—crucial in mmWave systems—because it operates in the digital domain and can be cascaded with RF-domain beamforming to reduce the number of required RF chains. Overall, this method directly addresses the geometric delay misalignment challenge highlighted in Section III. By realigning the LoS paths in time, it restores frequency-flatness across subcarriers, thereby enabling coherent combining and improving system performance.

## V. Received Signal and Compensation Strategies

This section derives the received signal expression under various phase compensation strategies to evaluate the impact of each phase component on system performance, particularly in terms of coherent combining and channel flatness.

### A. Received Signal Model and Zero-Forcing Equalization

At subcarrier $f$, the received signal $Y(f)$ results from the coherent superposition of signals transmitted by all APs and their antenna elements:

$$Y(f)=\left(\sum_{k\in\mathcal{S}}\sqrt{\mu_k}\sum_{i=1}^{N_{\text{Tx}}}W_i^k(f)H_i^k(f)\right)X(f)+N(f) \qquad (7)$$

where $W_i^k(f)$ is the beamforming coefficient at antenna $i$ of AP $k$, $\mu_k$ is a power scaling factor such that $\sum_{k\in\mathcal{S}}\mu_k=1$, and $N(f)$ is complex Gaussian noise with $N(f)\sim\mathcal{CN}(0,\sigma_n^2)$.

The term $W_i^k(f)$ plays a central role in the analysis, as it encapsulates all phase compensation strategies applied at the transmitter side. In the sequel, its expression will be varied to selectively correct different phase components of the channel (e.g., delay-induced, static, spatial), thereby enabling a systematic evaluation of their individual impact on the received signal and system performance.

To recover the transmitted symbol, ZF equalization is applied. The estimated composite channel is defined as:

$$E(f)=\sum_{k\in\mathcal{S}}\sqrt{\mu_k}\sum_{i=1}^{N_{\text{Tx}}}W_i^k(f)H_i^k(f) \qquad (8)$$

The channel is assumed to be perfectly estimated and used to compute the equalization factor $E(f)$, yielding the symbol estimate $\widehat{X}(f)=\frac{Y(f)}{E(f)}$. This model enables the evaluation of how different transmitter-side phase corrections—captured by the weights $W_i^k(f)$—affect the equalized signal quality and the resulting bit error rate (BER) across subcarriers.

### B. Phase Compensation Scenarios: Beamforming Strategies

This section outlines the transmitter-side compensation strategies evaluated in this work. Each strategy corresponds to a specific beamforming coefficient $W_i^k(f)$ in Eq. (7), targeting a subset of the LoS phase components defined in Section II.

The initial random phase offset of the LoS component (term [1] in Eq. (3)), due to CDL generation and polarization effects, is not corrected at the transmitter. It is removed by the ZF equalizer and thus excluded from the compensation strategies:

**No compensation:** All APs transmit the same symbol without applying any correction, i.e., $W_i^k(f)=1$. The LoS contributions arriving at the receiver are affected by differences in delay, static phase, and spatial alignment, resulting in phase misalignment across subcarriers.

**Frequency delay compensation:** Each AP applies $e^{j2\pi f(\tau_{\text{ref}}-\tau_{\text{LoS}}^k)}$ to cancel the delay-induced term [3], aligning LoS arrivals within the CP.

**Delay and static phase compensation:** A static phase correction $e^{j\frac{2\pi}{\lambda_0}d_k}$ is added to compensate term [2], ensuring both temporal and phase alignment of the LoS paths.

**Full phase compensation:** Per-antenna analog beam steering is added to correct the spatial term [4]. The frequency-dependent spatial term [5] is not addressed, as its effect is negligible in the considered scenario.

These strategies are designed to progressively mitigate the physical misalignments between distributed APs and analyze the contribution of each phase term to system performance.

## VI. Performance Evaluation

The performance of the proposed compensation strategies is evaluated via Monte Carlo simulations, using BER as the main metric under realistic propagation conditions. The simulation setup is summarized in Table I. The APs are placed at the vertices of an equilateral triangle (100 m side), centered around the UE. Each AP is located 10 m above ground and oriented toward the triangle's center. The channel is generated using the 3GPP CDL-D profile to reflect LoS-dominant propagation. Directional parameters are adjusted via coordinate transformations to ensure consistency with the actual AP–UE geometry. In the *full phase compensation* strategy, analog beam steering is applied per AP toward its dominant cluster, typically corresponding to the LoS direction. A fixed beam orientation is used across all subcarriers, consistent with mmWave analog hardware constraints.

To provide an upper bound, the performance of *Maximum Ratio Transmission* (MRT) is also shown. MRT uses fully digital beamforming with one RF chain per antenna, adapting both amplitude and phase per subcarrier:

$$W_i^k(f)=H_i^k(f)^*/\sqrt{\sum_{i=1}^{N_{\text{Tx}}}|H_i^k(f)|^2} \qquad (9)$$

Table I: Simulation Parameters for the Evaluated Scenario

| Parameter | Value |
|---|---|
| CDL-D Cross Polarization | 0 |
| Carrier Frequency ($f_c$) | 30 GHz |
| Number of Subcarriers | 2048 |
| Subcarrier Spacing ($\Delta f$) | 60 kHz |
| Number of AEs per AP ($N_{\text{Tx}}$) | 16 |
| Array Configuration | $4\times4$ URA |
| AE Pattern / Polarization | Omnidirectional / Horizontal |
| Number of AEs for UE | 1 |
| Number of APs ($K_{\mathcal{AP}}$) | 3 |
| Power Allocation ($\mu_k$) | Equal across APs |
| Delay Spread | 100 ns |
| Modulation | 16 QAM |
| UE Position $[x,y,z]$ (m) | [10,20,1.6] |
| UE Orientation $[\alpha, \beta, \gamma]$ (°) | [180, 0, 0] |

This maximizes SNR per subcarrier but is impractical in mmWave due to hardware cost. In our distributed setup, MRT is applied locally at each AP based on its own channel coefficients. For reference, we also report the performance of a centralized "global MRT" strategy, where all APs are jointly precoded using the aggregated channel.

Fig. 2 shows the BER versus $E_b/N_0$ for all strategies. As expected, the *no compensation* case exhibits poor performance due to cumulative misalignments in delay and phase, leading to destructive combining and strong frequency selectivity. Introducing *delay-only* correction yields a steep performance improvement—about 10 dB SNR gain at BER $= 10^{-2}$—by ensuring temporal alignment of LoS signals within the CP.

Further improvement is observed with *delay + static phase* compensation, yielding an additional 2.5 dB gain. This reflects the benefit of aligning constant phase offsets across APs, thereby enabling constructive interference across subcarriers. When spatial beam steering is also included (*full compensation*), the system closely approaches MRT performance, with a gap below 0.5 dB throughout the entire SNR range. Moreover, the results confirm that local MRT and global MRT yield nearly identical curves in this LoS-dominated scenario.

These results demonstrate that most of the performance gap with MRT can be closed through lightweight corrections of delay and static phase, combined with analog beam steering. The residual gap is primarily due to the absence of per-element digital precoding. Overall, the proposed method enables scalable, low-complexity transmission in distributed MISO-OFDM systems while achieving near-optimal performance.

The benefits of delay compensation depend on the UE's position relative to the APs. While some locations may naturally yield aligned LoS delays due to geometric symmetry, such cases are rare. In general, compensation is required to ensure robust performance across the coverage area.

## VII. Conclusion

This paper tackled the challenge of LoS delay misalignment in distributed MISO-OFDM systems. A phase decomposition of the LoS channel revealed the key contributions of delay, static distance, and antenna position to phase misalignment. To address these effects, we proposed a low-complexity, frequency-domain compensation technique that aligns LoS paths in time using per-subcarrier phase rotation. The method relies only on local delay knowledge, requires no central coordination, and remains compatible with analog beamforming—making it practical for mmWave systems.

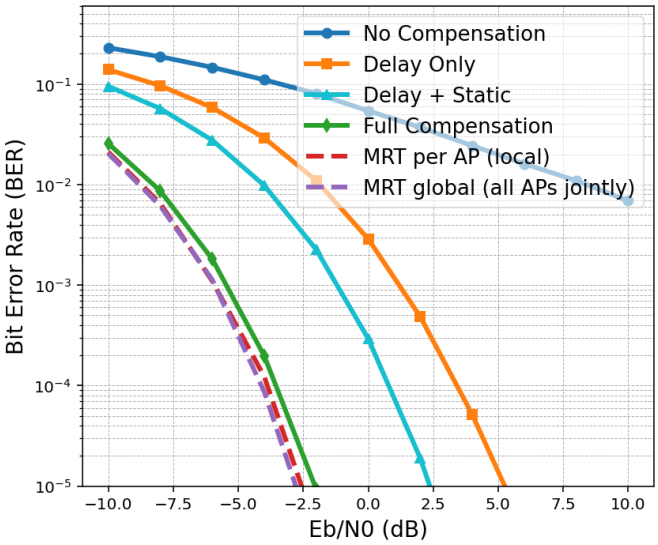


Figure 2: BER Performance for Different Phase Compensation Strategies

Simulation results show that correcting delay and static phase terms significantly improves BER, closely approaching the performance of full phase compensation. The approach is transparent to the receiver and scalable.

## References

[1] Z. Chen and E. Björnson, "Channel hardening and favorable propagation in cell-free massive MIMO with stochastic geometry," *IEEE Transactions on Communications*, vol. 66, no. 11, pp. 5205–5219, 2018.

[2] J. Zhang, S. Chen, Y. Lin, J. Zheng, B. Ai, and L. Hanzo, "Cell-free massive MIMO: A new next-generation paradigm," *IEEE Access*, vol. 7, pp. 99 878–99 888, 2019.

[3] Y. Li, C. Zhang, and Y. Huang, "Distributed beam selection for millimeter-wave cell-free massive MIMO based on multi-agent deep reinforcement learning," in *2024 IEEE Wireless Communications and Networking Conference (WCNC)*, 2024, pp. 1–6.

[4] N. Zhou, Z. Wang, C. Ma, Y. Huang, and Q. Shi, "Distributed precoder based on weighted MMSE with low complexity for massive MIMO systems," *IEEE Communications Letters*, vol. 29, no. 3, pp. 482–486, 2025.

[5] K.-M. Chen, Y.-H. Pan, and T.-S. Lee, "Low-complexity beam selection for hybrid precoded multi-user mmWave communications," in *2018 IEEE International Conference on Signal Processing, Communications and Computing (ICSPCC)*, 2018, pp. 1–5.

[6] T. Rolland, M. Crussière, and M. Le Bot, "BER prediction of distributed MISO systems using beamsteering with phase compensation in mmWave channels," *Proc. IEEE Vehicular Technology Conference (VTC Spring)*, 2025, in press.

[7] H. Cao, H. Zeng, X. Zhu, Q. Yang, and N. Wu, "Adaptive fuzzy logic based AP selection for scalable user-centric cell-free massive MIMO," *IEEE Transactions on Vehicular Technology*, vol. 74, no. 2, pp. 3429–3433, 2025.

[8] C. Wei, H. Tian, K. Xu, X. Xia, W. Xie, and C. Li, "A game-theoretic approach for user-centric AP selection in cell-free massive MIMO under dynamic user demand environment," *IEEE Wireless Communications Letters*, vol. 14, no. 3, pp. 876–880, 2025.

[9] 3rd Generation Partnership Project (3GPP), "Technical Specification Group Radio Access Network; Study on scenarios and requirements for next generation access technologies," 3GPP, TR 38.901, 2019.